Thermosolvatochromism of Betaine Dyes Revisited: Theoretical Calculations of the Concentrations of Alcohol−Water Hydrogen-bonded Species and Application to Solvation in Aqueous Alcohols

Erick L. Bastos, Priscilla L. Silva, and Omar A. El Seoud*

Instituto de Química, Universidade de São Paulo, C.P. 26077, 05513-970 São Paulo, S.P., Brazil

Received: April 11, 2006; In Final Form: May 23, 2006

Solvatochromic data of 2,6-diphenyl-4-(2,4,6-triphenylpyridinium-1-yl)phenolate (RB) in aqueous methanol, 1-propanol, 2-propanol, and 2-methyl-2-propanol at 25 °C were recalculated by employing a recently introduced model that explicitly considers the presence of 1:1 alcohol−water hydrogen-bonded species, ROH−W, *in bulk solution* and their exchange equilibria with water and alcohol in the probe solvation microsphere. The thermosolvatochromic behavior of RB in aqueous ethanol was measured in the temperature range from 10 to 60 °C; the results thus obtained were treated according to the same model. All calculations require reliable values of K_{dissoc}, the dissociation constant of the ROH−W species. This was previously calculated from the dependence of the density of the binary solvent mixture on its composition. Through the use of iteration, the volume of the hydrogen-bonded species, V_{ROH-W}, and K_{dissoc} are obtained *simultaneously* from the same set of experimental data. This approach may be potentially problematic because K_{dissoc} and V_{ROH-W} are highly correlated. Therefore, we introduced the following approach: (i) V_{ROH-W} was obtained from *ab initio* calculations, (ii) these volumes were corrected for the nonideal behavior of the binary solvent mixtures at different temperatures, (iii) corrected V_{ROH-W} values were employed as *a constant* in the equation used to calculate K_{dissoc} (from density vs binary solvent mixture composition). V_{ROH-W} calculated by the COSMO-RS solvation model fitted the density data better than those calculated by the IEFPCM model. In all aqueous alcohols, solvation by ROH−W is favored over that by the two precursor solvents. In aqueous ethanol, a temperature increase resulted in a gradual desolvation of RB, due to a decrease in the hydrogen-bonding of both components of the mixture. The microscopic polarities of ROH−W are much closer to those of the precursor alcohols.

Introduction

Note: A list of all abbreviations and symbols employed is given after the Conclusions.

The study of solvatochromism has contributed a great deal to our understanding of solvation. The UV−vis spectra, absorption or emission, of certain solvatochromic indicators (hereafter designated as "*probes*") were measured in solvents, and/or solvent mixtures, and the data thus obtained have been employed to analyze both solvent−probe and solvent−solvent interactions. The study of thermosolvatochromism adds the dimension of temperature to solvatochromism. Extensive use has been made of an empirical solvent polarity scale, E_T, calculated from $E_T = 28591.5/\lambda_{max}$ (nm). The latter scale converts the electronic transition within the probe into the corresponding intramolecular charge-transfer energy, E_T in kcal mol^{-1}.[1,2] In binary solvent mixtures of protic solvents, for example, alcohol, ROH, and water, W, the polarity has been rationalized in terms of the pK_a and hydrophilic/hydrophobic character of both probe and organic cosolvent. We have shown that thermosolvatochromic data in the above-mentioned binary solvent mixtures are best analyzed by considering that the medium is composed of three species, ROH, W, and a 1:1 hydrogen-bonded "complex" solvent ROH−W. Dependence of the density of the binary solvent mixture on its composition has been employed to calculate the equilibrium constant of dissociation, K_{dissoc}, of the ROH−W complex, from which the "effective" concentrations of the (three) solvent species in "bulk" mixture were obtained.[3−5]

The input data to calculate K_{dissoc} include the following: M_{ROH}, M_W, M_{ROH-W}, V_{ROH}, and V_W, along with initial estimates of K_{dissoc} and V_{ROH-W}.[6−8] Here, M and V refer to the molecular mass and molar volume of the solvent species, respectively. A reexamination of the density data published for mixtures of water and acetonitrile, methanol (MeOH) and tetrahydrofuran,[8] as well as the equation employed to calculate K_{dissoc} revealed that the latter constant and V_{ROH-W} are highly correlated, with correlation coefficients of $r > 0.97$. This is a typical example of multicollinearity, which has been discussed in detail elsewhere.[9] The consequences of multicollinearity include larger standard errors in the quantities calculated and lower statistical significance of the results, *independent* of the value of the regression coefficient. In limiting cases, several local minima, for example, of the residuals, may be obtained by iteration; these correspond to *noticeably different* combinations of the quantities calculated.[10] Additionally, the volume of the MeOH−W complex does not vary systematically as a function of increasing temperature; it increases then decreases as T is increased from 20 to 55 °C.[8] We were also faced with a similar problem for aqueous mixtures of 2-methyl-2-propanol (2-Me-2-PrOH).[11] The above-mentioned problems have prompted us to reexamine this very important aspect of binary solvent mixtures, namely, the formation and

* To whom correspondence should be addressed. Fax: 55-11-3091-3874. E-mail: elseoud@iq.usp.br.

10.1021/jp062250t CCC: $33.50
Published on Web 08/10/2006

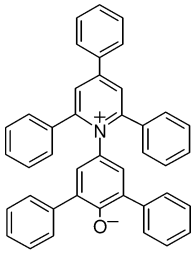

RB

Figure 1. Molecular structure of 2,6-diphenyl-4-(2,4,6-triphenylpyridinium-1-yl)phenolate, RB, the solvatochromic probe employed.

some properties of the ROH−W complexes formed, in particular their volumes and polarities.

We have developed a theoretical approach to calculate V_{ROH-W}, hence K_{dissoc} for mixtures of water with methanol, MeOH, ethanol, EtOH, 1-propanol, 1-PrOH, 2-propanol, 2-PrOH, and 2-methyl-2-propanol, 2-Me-2-PrOH, at different temperatures. The data calculated were applied to analyze solvatochromism of the probe 2,6-diphenyl-4-(2,4,6-triphenylpyridinium-1-yl)phenolate, RB (see structure in Figure 1), in binary solvent mixtures of water with these alcohols at 25 °C, as well as its thermosolvatochromism in aqueous ethanol, in the temperature range 10 to 60 °C. Theoretically calculated K_{dissoc} values are lower but correlated linearly with those previously calculated from density data. RB is preferentially solvated by all alcohols; increasing T of aqueous ethanol resulted in the desolvation of RB, due to the concomitant decrease of solvent structure. The polarities of the ROH−W are more similar to those of the precursor alcohols.

Experimental Section

Materials. RB was purchased from Merck. Commercial methanol and "absolute" ethanol (Valduto-Mensalão Química, DF) were further dried by distillation from the corresponding sodium alkoxide. The densities and $E_T(30)$ (polarity scale of RB) of both solvents were in excellent agreement with literature values.[1]

Densities of ROH−W Mixtures. These were determined for MeOH−W, EtOH−W, binary solvent mixtures by use of a DMA-40 resonating tube digital densimeter (Anton Paar, Graz). Densities of 1-PrOH−W, 2-PrOH−W, and 2-Me-2-PrOH−W were taken from literature.[3,12]

Spectrometric Determination of $E_T(30)$. Determination of $E_T(30)$ of ethanol−water mixtures was carried out as explained in detail elsewhere,[3−5] by using a Beckman DU-70 UV−vis spectrometer, equipped with a thermostated cuvette holder. The following information is relevant: final probe concentration, 2 to 5 × 10^{-4} mol L^{-1}; number of solvent samples measured = 18, including the two pure solvents; temperature control inside the holder, ±0.05 °C; number of scans = 2; scan rate = 120 nm min^{-1}. Values of λ_{max} were calculated from the first derivative of the absorption spectrum, the uncertainty in $E_T(30) \leq 0.2$ kcal mol^{-1}.

Quantum Chemical Calculations. The structures of alcohols, water, and alcohol−water complexes were optimized *without constrains* by using the density functional theory (DFT) at Becke's three parameter hybrid functional, using the correlation functional of Lee, Yang, and Parr (B3LYP) with the 6-31+G(3d,p) basis set.[13,14] Stationary points were confirmed as minima via vibrational frequency calculations. Optimized geometries were used to calculate the solvent accessible volumes using both the conductor-like screening model for real solvents (COSMO-RS) and the integral equation formalism (IEFPCM) polarizable continuum models with the 6-31+G(3d,p) basis set.[15−17] *Ab initio* calculations were performed by using the Gaussian 03 program package.[18] Three-dimensional structures and surfaces were calculated by using ArgusLab 4.0.1 software.[19] All calculations were performed at the advanced computing facilities (LCCA) of the University of São Paulo.

Results and Discussion

RB is probably the most studied probe, both in pure solvents and in their mixtures. Consequently, it is appropriate to reexamine some of our previous data of this probe in ROH−W mixtures. The reason is that simpler solvation models have been applied for aqueous MeOH, no complex solvent was considered; for the other alcohols, the formation of ROH−W was restricted to the solvation microsphere, that is, the presence of hydrogen-bonded species in bulk mixture was ignored.[20−25] The solvation model that we have recently introduced explicitly considers the exchange equilibria of all solvent species present, namely, ROH, W, and ROH−W, as shown by the following equations[3]

$$\mathrm{ROH} + \mathrm{W} \rightleftharpoons \mathrm{ROH\text{-}W} \quad (1)$$

$$\mathrm{Probe(ROH)}_m + m\mathrm{W} \rightleftharpoons \mathrm{Probe(W)}_m + m\mathrm{ROH} \quad (2)$$

$$\mathrm{Probe(W)}_m + m(\mathrm{ROH-W}) \rightleftharpoons \mathrm{Probe(ROH-W)}_m + m\mathrm{W} \quad (3)$$

$$\mathrm{Probe(ROH)}_m + m(\mathrm{ROH-W}) \rightleftharpoons \mathrm{Probe(ROH-W)}_m + m\mathrm{ROH} \quad (4)$$

where m represents the number of solvent molecules whose exchange, in the probe solvation microsphere, affects E_T; *the value of m should not be confused with the total number of molecules that solvate the probe*. An important consequence of eqs 1−4 is that the observed E_T (E_T^{obs}) is given as the sum of the polarities of the solvent species present, E_T^W, E_T^{ROH}, and E_T^{ROH-W}, multiplied by the corresponding mole fraction in the solvation microsphere, χ_W^{Probe}, χ_{ROH}^{Probe}, and χ_{ROH-W}^{Probe}, respectively. The latter are based on *effective, not analytical*, concentrations of alcohol and water in the bulk mixture

$$E_T^{obs} = \chi_W^{Probe} E_T^W + \chi_{ROH}^{Probe} E_T^{ROH} + \chi_{ROH-W}^{Probe} E_T^{ROH-W} \quad (5)$$

The relationship between bulk solvent composition and that of the microsphere is given by the so-called solvent "fractionation factors", defined by

$$\varphi_{W/ROH} = \frac{\chi_W^{Probe}/\chi_{ROH}^{Probe}}{(\chi_W^{Bk;Effective}/\chi_{ROH}^{Bk;Effective})^m} \quad (6)$$

$$\varphi_{ROH-W/ROH} = \frac{\chi_{ROH-W}^{Probe}/\chi_{ROH}^{Probe}}{(\chi_{ROH-W}^{Bk;Effective}/\chi_{ROH}^{Bk;Effective})^m} \quad (7)$$

$$\varphi_{ROH-W/W} = \frac{\chi_{ROH-W}^{Probe}/\chi_W^{Probe}}{(\chi_{ROH-W}^{Bk;Effective}/\chi_W^{Bk;Effective})^m} = \frac{\varphi_{ROH-W/ROH}}{\varphi_{W/ROH}} \quad (8)$$

where Bk refers to bulk mixture and χ is that defined before. In eq 6, $\varphi_{W/ROH}$ (W substituting ROH) describes the composition of the probe microsphere, relative to that of the bulk mixture. For $\varphi_{W/ROH} > 1$, the microsphere is richer in W than the bulk

mixture; the converse holds for $\varphi_{W/ROH} < 1$, that is, the probe is preferentially solvated by ROH. Finally, a solvent fractionation factor of unity indicates an ideal behavior, that is, the microsphere and bulk mixture have equal compositions. The same line of reasoning applies to $\varphi_{ROH-W/ROH}$ (complex solvent substituting ROH) and $\varphi_{ROH-W/W}$ (complex solvent substituting W), eqs 7 and 8, respectively.

Treatment of solvatochromic data involves the following steps:[3-5] (i) calculation of V_{ROH-W} and K_{dissoc} from the dependence of densities of the binary solvent mixtures on their composition, (ii) calculation (based on K_{dissoc}) of effective χ_{ROH}, χ_W, and χ_{ROH-W} for the different solvent mixtures employed, and (iii) calculation of the corresponding $\varphi_{W/ROH}$, $\varphi_{ROH-W/ROH}$, and $\varphi_{ROH-W/W}$ from the dependence of E_T^{obs} on solvent composition, by employing eq 9

$$E_T^{obs} = \frac{(\chi_{ROH}^{Bk;Effective})^m E_T^{ROH} + \varphi_{W/ROH}(\chi_W^{Bk;Effective})^m E_T^W + \varphi_{ROH-W/ROH}(\chi_{ROH-W}^{Bk;Effective})^m E_T^{ROH-W}}{(\chi_{ROH}^{Bk;Effective})^m + \varphi_{W/ROH}(\chi_W^{Bk;Effective})^m + \varphi_{ROH-W/ROH}(\chi_{ROH-W}^{Bk;Effective})^m} \quad (9)$$

The derivation of this and other equations related to the treatment of solvatochromic data has been given in detail elsewhere and will not be repeated in the text.[3-5] For clarity, however, some of these derivations are included in the Supporting Information, SI. It is worthwhile to stress that the input data include experimentally determined E_T^{obs}, $E_T(30)$ROH, and $E_T(30)$W and calculated $\chi_W^{Bk;Effective}$, $\chi_{ROH}^{Bk;Effective}$, and $\chi_{ROH-W}^{Bk;Effective}$. Values of $\varphi_{W/ROH}$, $\varphi_{ROH-W/ROH}$, and E_T^{ROH-W} are then calculated from eq 9. Iteration is continued until the (complex) dependence of E_T^{obs} on χ_W (usually a polynomial of the fourth to sixth power) is satisfactorily reproduced. The criteria for the goodness of fit include an acceptably small value of χ^2 (usually $\leq 10^{-6}$) and an agreement between calculated and experimental values E_T(probe)ROH and E_T(probe)W.[3-5] Finally, $\varphi_{ROH-W/W}$ is calculated by dividing $\varphi_{ROH-W/ROH}$ by $\varphi_{W/ROH}$. The preceding discussion underlines the importance of calculation of K_{dissoc}, based on a reliable value of V_{ROH-W}. It also raises interest in comparing the polarities of ROH-W with those of ROH and W.

At the outset, it is appropriate to address the use of 1:1 stoichiometry for ROH−W, according to eq 1. This is a practical and convenient assumption because it renders subsequent calculations tractable; it has been extensively employed by others to describe solvatochromism.[21-26] Mixed solvent species with stoichiometry other than 1:1 may be treated, to a good approximation, as mixtures of the 1:1 structure plus excess of a pure solvent. The formation of ROH−W complexes are manifested by the nonideal, that is, nonlinear relationships between compositions and physicochemical properties of binary solvent mixtures, including their densities, dielectric constants, NMR relaxation times, dielectric relaxations, and fluorescence lifetimes of dissolved probes.[27-31] Theoretical calculations, the Kirkwood−Buff integral functions (that describe W−W, ROH−ROH, and ROH−W interactions), and electron-impact mass spectroscopy support the formation of ROH−W complexes.[32-34] Additionally, the 1:1 model has been successfully employed to fit the data of spectroscopic techniques that are particularly suitable to determine the stoichiometry of ROH−W aggregates, including the dependence of the ^{1}H chemical shift (NMR) and/or the peak area and frequency of $\tilde{\nu}_{OH}$ (FTIR) on [W].[35-37] When ^{1}H NMR spectroscopy is used, the stoichiometry of mixtures of dipolar aprotic solvents and water (in CCl_4) has been calculated; both 1:1 and 2:1 solvent−W complexes were considered. The ratios $K_{1:1}/K_{2:1}$ ranged from 26 (acetonitrile) to 132 (DMSO).[38] In summary, our solvatochromic data can be conveniently analyzed by considering 1:1 ROH−W complexes only.

TABLE 1: Selected Geometric Parameters and Dipole Moments of the 1:1 Alcohol−Water Hydrogen-bonded Complexes, Calculated by the B3LYP/6-31+G(3d,p) Basis Set[a]

complex	d(HO···H$_w$···O(H)R) (Å)	∠(O···H$_w$···O(H)R) (deg)	μ_{vacuum} (D)
MeOH−W	1.918	170.59	2.5161
EtOH−W	1.916	170.69	2.7056
1-PrOH−W	1.914	171.84	2.9040
2-PrOH−W	1.909	171.82	2.6517
2-Me-2-PrOH−W	1.906	171.58	2.5701

[a] d(HO···H$_w$···O(H)R) refers to the distance between the OH of water and the H-atom that is being transferred to the (O) atom of alcohol; the corresponding angle between the two oxygen atoms is given by ∠(O···H_w···O(H)R). For all complexes examined, the point group is C_1.

The ensuing discussion is organized as follows: calculation of optimized V_{ROH-W}, calculation of K_{dissoc} for ROH−W of the above-mentioned alcohols, and application to our previous and new solvatochromic data of RB.

Calculation of V_{ROH-W}. Briefly, the theoretical calculation of the molar volumes of 1:1 ROH−W complexes is based on geometry optimization of the precursor components (ROH and W) and of the 1:1 ROH−W complex, followed by calculation of their molar volumes at different temperatures. This procedure is detailed below.

Geometry Optimization. The level of theory chosen to optimize the geometry of ROH−W complexes was based on obtaining satisfactory data for water, including its dipole moment (μ) and energy of dimerization (ΔE_W), both quantities have been measured experimentally. Use of DFT with B3LYP functional and the 6-31+G(3d,p) basis set resulted in a $\mu_{(W)} = 1.885$ D and $\Delta E_W = -4.81$ kcal mol^{-1}; in good agreement with experimental values, $\mu_{(W)} = 1.854$ D and $\Delta E_W = -4.9$ to -5.2 kcal mol^{-1}.[39] Use of the 6-31+G(3d,p) basis set gave better results than those calculated with the more popular, although smaller basis sets, including B3LYP/6-31G(d,p): $\mu_{(W)} = 2.044$ D and $\Delta E_W = -7.54$ kcal mol^{-1} and B3LYP/6-31+G(d,p): $\mu_{(W)} = 2.195$ D and $\Delta E_W = -6.04$ kcal mol^{-1}.[39] Use of the 6-31+G(3d,p) basis set also gave satisfactory μ values for the alcohols studied (see Table SI-1 of the SI).

Both alcohol and water can act as a hydrogen-bond donor and/or hydrogen-bond acceptor. Theoretical calculations and microwave rotation tunneling spectroscopy have shown that the MeOH−W complex is energetically more favored (by ca. 1 kcal mol^{-1}) when methanol is acting as a hydrogen-bond acceptor.[40] This arrangement was employed with other alcohols since they are more basic than methanol. The distances, angles, and dipole moments, μ, that characterize the ROH−W complexes are listed in Table 1. As expected,[41] the HO···H$_w$···O(H)R hydrogen bonds are almost linear for all complexes. Full three-dimensional representations of these complexes are shown in Figure SI-1 of the SI.[42]

Calculation of the Solvent Molar Volume. To calculate the cavity volume occupied by ROH in a water continuum, we have employed both COSMO-RS and IEFPCM models with the B3LYP/6-31+G(3d,p) basis set. In both cases, surface excluded cavities were calculated by applying the united-atom topological model to atomic radii defined by the UFF force field. The

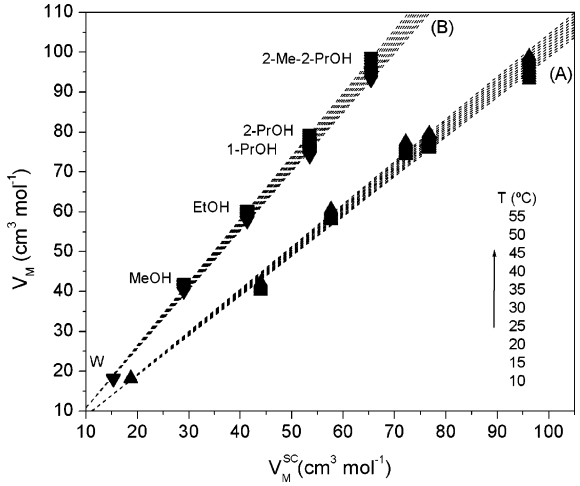

Figure 2. Relationship between experimentally determined molar volumes of solvents, V_M, and calculated molar volumes, V_M^{SC}, using (A, ▲) IEFPCM/B3LYP/6-31+G(3d,p) and (B, ▼) COSMO-RS/B3LYP/6-31+G(3d,p) for water and alcohols. For each solvent, the spread of V_M (at each V_M^{SC}) covers the temperature range 10−55 °C. For the COSMO-RS model, the points for 1-PrOH and 2-PrOH are much closer than those in the IEFPCM counterpart.

TABLE 2: Molar Volumes (V_M^{SC}, in cm^3 mol^{-1}) of W, ROH, and ROH−W, Obtained with Two Solvation Models Using the B3LYP/6-31+G(3d,p) Basis Set

solvent/ROH−W	V_M^{SC}, COSMO-RS	V_M^{SC}, IEFPCM
water	15.30	18.70
MeOH	29.00	43.96
EtOH	41.28	57.65
1-PrOH	53.47	72.18
2-PrOH	53.44	76.68
2-Me-2-PrOH	65.43	96.19
MeOH−W	42.93	61.78
EtOH−W	55.22	75.96
1-PrOH−W	67.44	90.44
2-PrOH−W	67.34	94.89
2-Me-2-PrOH−W	79.23	113.34

solvent cavity volumes thus obtained (V_{SC} in Å^3) were converted into molar volumes (V_M^{SC}, in cm^3 mol^{-1}) by multiplying it by Avogadro's number and dividing by 10^{24} (the latter operation converts Å^3 into cm^3). The same approach was applied in calculation of the ROH−W cavity volume. Table 2 shows the values calculated with both models for W, ROH, and ROH−W, respectively.

Calculation of the Molar Volumes of ROH−W at Different Temperatures and Correction of the Volumes thus Obtained due to the Nonidealities of the Binary Solvent Mixtures. The calculations that originated the data of Table 2 have no provision for the following: (i) effects of temperature on the volume of ROH−W and (ii) the nonidealities of the binary solvent mixtures. In principle, it is possible to employ molecular dynamics to calculate *T*-dependent molecular surfaces and cavities of ROH-W; see point (i).[43] Since this is a costly procedure (in terms of CPU time), we assumed that the dependence of the volume of ROH−W on temperature follows the same equation of the precursor pure liquids.[44] The procedure employed was as follows: (theoretical) V_M^{SC} of pure liquids (Table 2) were plotted against their experimental, density-based molar volumes, V_W and V_{ROH}, in the temperature range 10−55 °C, using 5 °C intervals (Figure 2). Temperature-dependent volumes of ROH−W were then calculated by using the *same* regression coefficients of the resulting 20 linear correlations (2 solvation models, 10 temperatures). Equation 10 shows a typical

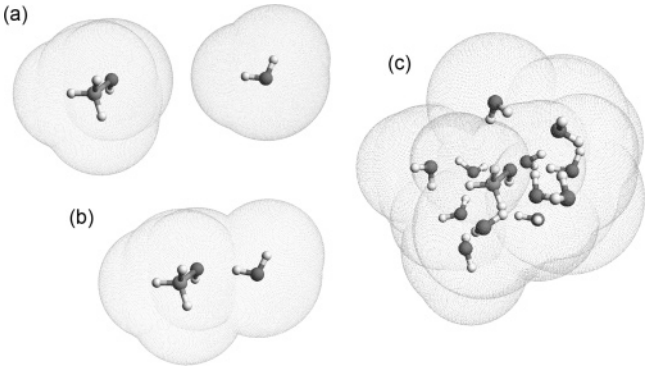

Figure 3. Solvent accessible surfaces of (a) separated methanol and water molecules, (b) the isolated MeOH−W complex, and (c) one MeOH−W solvated by 11 water molecules.

correlation, calculated by the COSMO-RS model for the data at 25 °C. The full set of linear equations is listed in Table SI-2.

$$V_M = -4.26359(\pm 1.2005) + 1.51271(\pm 0.02602)V_M^{SC}$$
$$r = 0.9994; \quad SD = 1.0688 \qquad (10)$$

The volumes calculated in the preceding step refer to *isolated* ROH−W species, that is, they do not consider volume changes due to the presence of these species in bulk nonideal solvent mixtures; see point (ii). This limitation is depicted qualitatively in Figure 3, where part a represents isolated molecules of MeOH and W. The combined volume of this (separated) solvent pair is 73.57 Å^3, compared with 71.30 Å^3 of part b. The latter refers to the volume of an isolated MeOH−W complex. This volume contraction (3%, COSMO-RS) is even more significant if one considers the effect of the surrounding species (W, MeOH, and MeOH−W) on MeOH−W complex in bulk solution. Part c of Figure 3 shows the solvation of one ROH−W by 11 W molecules. Again, the combined volume of *isolated* solvent species is 353.12 Å^3, compared with 329.15 Å^3 for the optimized geometry (7% reduction, COSMO-RS). This volume contraction continues for larger assemblies of solvent molecules. In conclusion, a correction for the nonadditivity of volumes is required.

Since the nonideal behavior of (bulk) binary solvent mixtures can be expressed in terms of an excess function, we decided to correct the above-mentioned volumes of ROH−W by adding the appropriate excess volumes. These are defined as the differences between experimental and expected molar volumes (the latter for an ideal mixture), expressed on the volume fraction scale (α) by eq 11

$$V_M^{E,\alpha} = V_M - [\alpha_W V_W + \alpha_{ROH} V_{ROH}] \qquad (11)$$

where (experimental) V_M is defined on the volume fraction scale by eq 12, where ρ is the density.[45]

$$V_M = \frac{\alpha_W \rho_W + \alpha_{ROH} \rho_{ROH}}{\rho[\alpha_W \rho_W M_W{}^{-1} + \alpha_{ROH} \rho_{ROH} M_{ROH}{}^{-1}]} \qquad (12)$$

The reason for expressing the volume excess function in terms of volume fraction rather than the mole fraction[46] is because the former scale is employed in the calculation of K_{dissoc}.[6−8] Figure 4 shows the dependence of the excess volumes of aqueous ethanol ($V_M^{E,\alpha}$) on the volume fraction of EtOH (α_{EtOH}) in the temperature range 10−40 °C. The vertical, dashed line corresponds to the solvent composition where the mole fraction of EtOH is 0.5, that is, where the stoichiometry of alcohol−water is 1:1. The corresponding excess volumes were employed

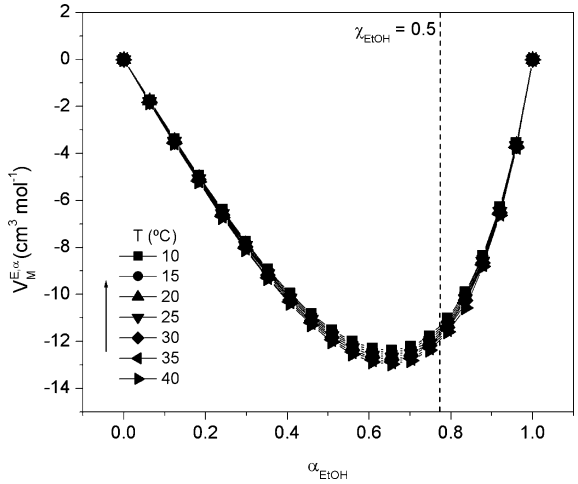

Figure 4. Dependence of the excess volume ($V_M^{E,\alpha}$) of aqueous ethanol on the volume fraction of the alcohol, α_{EtOH}, at different temperatures. The vertical, dashed line is that where the mole fraction of EtOH is 0.5, that is, where the stoichiometry of alcohol−water is 1:1.

to correct (ROH−W) volumes of the preceding step, at different temperatures; this procedure was employed throughout. The excess volumes calculated at different temperatures (where density data are available) and V_{ROH-W}, corrected for the effects of temperature and mixture nonideality, are listed in Table SI-3 of the SI.

Determination of the Alcohol−Water Association Constant (K_{assoc}) from Density Data. By considering that a mixture of water and a solvent is made of both components and the 1:1 solvent−water complex, Scott et al. have derived an equation to fit density data as a function of solvent volume fraction (eq 13).[6,7] Nonlinear fitting of experimental data calculates, simultaneously, V_{ROH-W} and K_{dissoc}.

$$\rho = \frac{[W]M_W + [ROH]M_{ROH} + [ROH - W]M_{ROH-W}}{[W]V_W + [ROH]V_{ROH} + [ROH - W]V_{ROH-W}} \quad (13)$$

As mentioned earlier, K_{dissoc} and V_{ROH-W} are highly correlated; their calculation from the same set of data may be suspect because of this multicollinearity. Use of V_{ROH-W}, *calculated by an independent method and employed as a fixed parameter in eq 13*, eliminates this problem and provides reliable dissociation constants. The V_{ROH-W} obtained from both IEFPCM and COSMO-RS models (Table SI-3 of the SI) were used in eq 13 to fit experimental data. In general, the fit of the IEFPCM model to the data was worse ($r^2 \leq 0.93$) than that of COSMO-RS ($r^2 \geq 0.998$ and $\chi^2 < 5 \times 10^{-6}$), so that the latter model was used throughout. Figure 5 shows the typical results of employing eq 13 to fit the density vs composition data, whereas the K_{dissoc} values calculated are reported in Table 3. An attempt to calculate K_{dissoc} by employing $V_{ROH-W} = V_{ROH} + V_W$ (taken from Table 2) showed that this approach is inadequate; the model simply does not fit the density data.

TABLE 3: Dependence of the Dissociation Constants of Alcohol−Water Complexes, K_{dissoc}, on Temperature

T (°C)	ROH−W	V_{ROH-W} (cm^3 mol^{-1})	K_{dissoc} [a]	r^2	$10^6 \times \chi^2$
10	EtOH−W	66.37	0.03007	0.9994	2.27
15	EtOH−W	66.73	0.03067	0.9995	1.74
	2-PrOH−W	77.50	0.06245	0.9989	4.32
20	EtOH−W	67.09	0.03134	0.9996	1.32
25	MeOH−W	55.33	0.00455	0.9997	0.92
			(0.0058)		
	EtOH−W	67.47	0.03187	0.9997	1.08
			(0.0357)		
	1-PrOH−W	79.68	0.08399	0.9994	2.95
			(0.0813)		
	2-PrOH−W	78.41	0.06494	0.9992	3.34
			(0.1237)		
	2-Me-2-PrOH−W	88.60	0.10104	0.9994	2.63
			(0.1429)		
30	EtOH−W	67.85	0.03247	0.9998	0.86
	1-PrOH−W	80.17	0.08702	0.9995	2.55
35	MeOH−W	55.90	0.00461	0.9995	2.14
	EtOH−W	68.23	0.03284	0.9997	1.12
	1-PrOH−W	80.67	0.08953	0.9995	2.51
	2-PrOH−W	79.29	0.06720	0.9993	3.09
	2-Me-2-PrOH−W	89.57	0.10275	0.9995	2.47
40	MeOH−W	56.15	0.00464	0.9994	2.29
	EtOH−W	68.62	0.03336	0.9997	0.96
	1-PrOH−W	81.16	0.09313	0.9997	1.47
	2-PrOH−W	79.74	0.06886	0.9993	2.99
	2-Me-2-PrOH−W	90.07	0.10428	0.9995	0.70
50	1-PrOH−W	82.19	0.09844	0.9996	1.89
	2-PrOH−W	80.73	0.07166	0.9994	2.53
	2-Me-2-PrOH−W	91.05	0.10522	0.9997	1.26

[a] Values in parentheses refer to K_{dissoc} values that were previously calculated from density data, where V_{ROH-W} (eq SI-9) was employed as an adjustable parameter.

The data of Table 3 show that although *ab initio*-based K_{dissoc} values at 25 °C are somewhat different from those previously

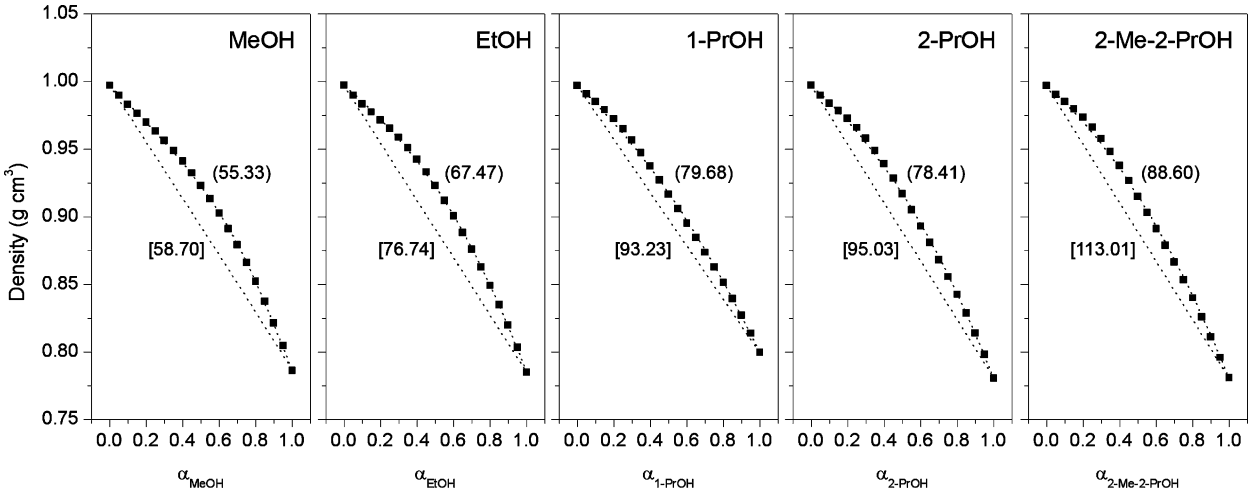

Figure 5. Representative plots showing the dependence of solution density on the volume fraction of ROH in ROH−W mixture at 25 °C. The solid squares are experimental data; the dashed curves show the fits obtained by the procedure outlined using V_M (in parentheses) and $V_W + V_{ROH}$ (in brackets).

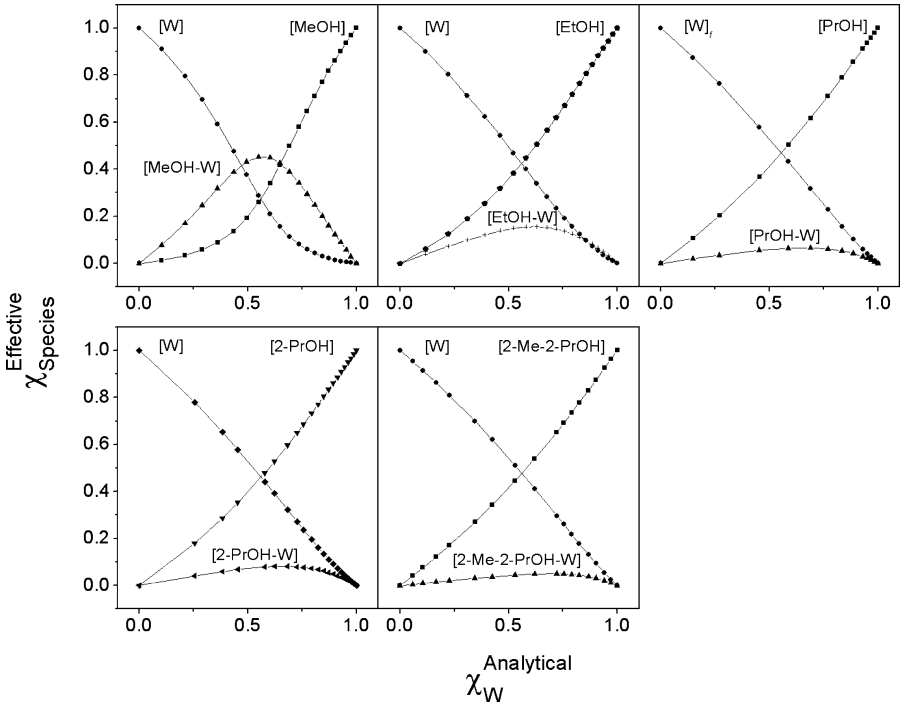

Figure 6. Species distribution at 25 °C for mixtures of water with MeOH, EtOH, 1-PrOH, 2-PrOH, and 2-Me-2-PrOH, respectively.

TABLE 4: Analysis of Solvatochromic Data in Binary ROH−W Mixtures at 25 °C[a]

ROH	*m*	$\varphi_{W/ROH}$	$\varphi_{ROH-W/ROH}$	$\varphi_{ROH-W/W}$	$E_T(30)$ W	$E_T(30)$ ROH	$E_T(30)$ ROH−W	r^2	χ^2
MeOH	1.352	0.466	3.212	6.892	63.086	55.396	56.703	0.9990	0.00717
EtOH	1.356	0.394	13.868	35.153	63.126	52.148	53.871	0.9990	0.01532
1-PrOH	1.695	0.263	184.41	701.21	63.167	50.582	52.600	0.9989	0.01639
2-PrOH	1.331	0.267	30.540	114.46	63.107	48.287	51.605	0.9995	0.01134
2-Me-2-PrOH	1.052	0.389	25.390	65.244	63.146	44.677	49.501	0.9984	0.05082

[a] $E_T(30)$ values reported were calculated by regression of $E_T(30)$ vs solvent composition. Experimental $E_T(30)_{Solvent}$ − calculated $\Delta E_T(30)_{Solvent}$ was within 0.1 kcal mol^{-1}.

TABLE 5: Thermosolvatochromic Data of RB in EtOH−W Mixtures

T (°C)	*m*	$\varphi_{W/ROH}$	$\varphi_{ROH-W/ROH}$	$\varphi_{ROH-W/W}$	E_T^W	E_T^{ROH}	E_T^{ROH-W}	r^2	χ^2
10	1.574	0.345	21.213	61.488	63.433	52.126	53.713	0.9988	0.01144
25	1.356	0.394	13.868	35.153	63.126	52.148	53.871	0.9990	0.01532
40	1.218	0.463	9.845	21.263	62.799	51.564	53.136	0.9984	0.02553
60	1.171	0.541	7.364	13.621	62.187	50.633	51.810	0.9997	0.00502

calculated, both sets of results show linear correlation with $r = 0.905$; r increases to 0.961 if the point of 2-PrOH is eliminated. As expected, K_{dissoc} increases (i.e., ROH−W association decreases) as a function of increasing temperature; the van't Hoff equation applies satisfactorily to all alcohols. Figure SI-2 of the SI, that is, the corresponding ΔC_p is essentially temperature independent in the *T*-range studied, in agreement with published data.[47−49]

The *effective* mole fractions of water ($\chi_W^{Bk;Effective}$), alcohol ($\chi_{ROH}^{Bk;Effective}$), and the 1:1 water−alcohol complex ($\chi_{ROH-W}^{Bk;Effective}$) were calculated from eqs 5, 6, and 7, as reported elsewhere;[3] the results are graphically represented in Figure 6. Interestingly, this figure shows that the maximum χ_{ROH-W} is more sensitive to the volume of ROH than to its pK_a. The fact that more basic alcohols do not bind more strongly to water shows that increasing the chain length of the alkyl group attenuates hydrogen bonding due to the following: (a) an increase in hydrophobic interactions, whose relative importance increases rapidly as a function of increasing the volume of R, and (b) an increase in the number of thermal collisions between W and ROH that are required for H-bond formation. The latter entails an increase in the time required for the alcohol molecule to assume a favorable orientation for hydrogen bonding with water.[31,37,50−52] It is worth mentioning that our previous data also indicated that probe−solvent interactions are rather sensitive to its hydrophobic interactions with the organic component of the binary solvent mixture.[3−5]

Effective mole fractions and observed values of $E_T(30)$ were used to calculate *m*, the different φ, and E_T^{ROH-W} for five aqueous alcohols at 25 °C and for aqueous ethanol in the temperature range 10−60 °C (eq 9). The results of these calculations are listed in Tables 4 and 5, respectively, whereas Figure 7 shows the $E_T(30)$/temperature/solvent composition contours for EtOH−W.

Regarding these results, the following is relevant:

(i) Using the new set of K_{dissoc}, we recalculated 17 previous data sets for W−ROH mixtures, for four different zwitterionic probes, at 10−60 °C.[3−5,11] The percent differences obtained ($\sqrt{\{\Sigma}$ (difference between values using the two $K_{dissoc})^2\}/17) \times 100$) were as follows: 0.4%, *m*; 5.4%, $\varphi_{W/ROH}$; 11.9%, $\varphi_{ROH-W/ROH}$; 7.7%, $\varphi_{ROH-W/ROH}$; 0.13%, E_T(ROH−W); 0.05% in both E_T(W) and E_T(ROH). These results are satisfying because the differences are small. More importantly, there was not a single case where the previously determined order of

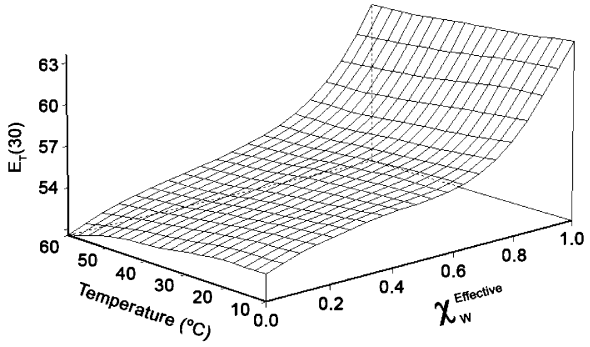

Figure 7. Solvent polarity/temperature/solvent composition contours for RB in EtOH−W.

preferential solvation was inversed, namely, ROH > W, ROH−W > W, and ROH (results of calculations not listed). Consequently, use of the new of K_{dissoc} does not entail any revision of our previous conclusions regarding thermosolvatochromism.

(ii) The quality of our data is shown by the values of χ^2 and r^2 and by the excellent agreement between calculated and experimental $E_T(30)$ROH and $E_T(30)$W, respectively. The polynomial dependence of observed $E_T(30)$ on χ_W, at 25 °C, has been reported elsewhere.[20] The corresponding dependence for EtOH, as a function of temperature is reported in Table SI-4 of the SI.

(iii) Figure 7 and all other plots of $E_T(30)$ vs solvent composition (not shown) indicate that RB is preferentially solvated by ROH, in agreement with the very low solubility of this probe in water, 7.2×10^{-6}.[1]

(iv) In discussing φ, it should be born in mind that the zwitterionic form of the probe is the solvatochromic one, that is, the probe acts as the hydrogen-bond acceptor through its phenolate oxygen.[53] There are also hydrophobic interactions between the probe and the alkyl chain of the alcohol (either pure or as ROH-W). Therefore, preferential solvation is expected to depend on the pK_a and hydrophilic/hydrophobic character of both the probe and the alcohol. Where these two properties are compared, we restrict our discussion to MeOH, EtOH, and 1-PrOH, to avoid complications due to steric effects (in the case of 2-PrOH and 2-Me-2-PrOH).[4]

(v) For all alcohols, and for EtOH−W at all temperatures, $\varphi_{W/ROH} < 1$. This indicates that the alcohol is always favored in the competitive solvation by pure solvents. The importance of RB−ROH hydrophobic interactions is shown in Table 4, where the order of $\varphi_{W/ROH}$ is (MeOH) > (EtOH) > (1-PrOH), that is, the longer the chain length of the alcohol, the higher is its preferential solvation of RB. The pK_a values of these alcohols are 15.5, 15.9, and 16.1, respectively.[54] Hydrogen-bond donation to the phenolate oxygen of RB decreases as a function of increasing the pK_a of the alcohol, that is, the order of $\varphi_{W/ROH}$ should have been the inverse. This attenuation of hydrogen bonding, however, is more than compensated for by probe−ROH hydrophobic interactions.

(vi) Regarding the fractionation factors of ROH−W of Table 4, the following can be observed: (a) All $\varphi_{WROH-W/ROH}$ and $\varphi_{WROH-W/W}$ values are >1; (b) all $\varphi_{WROH-W/ROH}$ values are $< \varphi_{WROH-W/W}$; (c) the order for both fractionation factors is MeOH < EtOH < 1-PrOH. Point (a) indicates that RB is preferentially solvated by ROH-W. Point (b) shows that ROH−W is more efficient in displacing water than alcohol from the probe solvation microsphere. Since the alcohols employed are more basic than water, we can assume that the structure of the complex species is given by the following: $H_w-O-H\cdots O(R)H_{ROH}$, that is, the two hydrogen atoms marked in *italic* are the sites for hydrogen bonding with the probe phenolate oxygen. As argued elsewhere, this ROH−W association partially deactivates H_w toward further hydrogen bonding, this deactivation is greater the stronger the basicity of the alcohol.[55,56] This conclusion has been recently corroborated by FTIR work on aqueous mixtures of 1-PrOH. Thus, the frequencies of the stretching and deformation vibration modes of H_w of the hydrate are both blue-shifted relative to the corresponding frequencies of bulk water.[37] Point (c) shows that preferential solvation by ROH−W increases as a function of increasing the hydrophobicity of its organic component. This conclusion agrees with the order of $\varphi_{W/ROH}$ discussed above and with the fact that $\varphi_{ROH-W/W} > \varphi_{ROH-W/ROH}$. This is because $\varphi_{ROH-W/W}$ is related to the difference between hydrogen bonding plus hydrophobic interactions of ROH−W vs only hydrogen bonding by water (see eq 3). On the other hand, both hydrogen-bonding and hydrophobic interactions contribute to solvation by the two solvents that define $\varphi_{ROH-W/ROH}$ (see eq 4).

(vii) Examination of thermosolvatochromism in aqueous ethanol, Table 5, shows that a temperature increase results in a *decrease* of *m*, $E_T(30)_{EtOH}$, $E_T(30)_W$, $\varphi_{ROH-W/ROH}$, and $\varphi_{ROH-W/W}$ and an *increase* of $\varphi_{W/ROH}$. The decrease in polarities of the pure solvents can be attributed to a decrease of solvent stabilization of the probe ground state, as a result of the concomitant decrease of solvent structure and hydrogen-bonding ability.[28,57] Preferential "clustering" of water and alcohol as a function of increasing temperature means that the strength of ROH−W interactions also *decreases* in the same direction,[28,34,58,59] with a concomitant decrease in its ability to displace both water and alcohol. This explains the decrease of $\varphi_{ROH-W/ROH}$ and $\varphi_{ROH-W/W}$ as a function of increasing temperature. It is known that the structure of water is less affected by increasing temperature than that of alcohols.[34] That is, hydrogen bonding of water with the probe ground state is less susceptible to temperature increase than that of its ROH counterpart. This leads to a measurable "depletion" of ROH in the probe solvation microsphere at higher temperatures, so that $\varphi_{W/ROH}$ increases as a function of increasing temperature.

(viii) The fact that *all* $E_T(30)$ROH−W are much closer to $E_T(30)$ROH than to $E_T(30)$W is interesting and may be taken to indicate that the properties of this mixed species is dominated by those of the alcohol. This conclusion is corroborated by the fact that $\varphi_{W/ROH}$ is less than unity, and all $\varphi_{WROH-W/ROH}$ values are $< \varphi_{WROH-W/W}$. It is possible that this susceptibility to solvation by the alcohols is somewhat enhanced because of the very hydrophobic character of RB.

Conclusions

Thermosolvatochromism in binary solvent mixtures can be described by a model based on exchange equilibria between the species present in solution (W, ROH, ROH−W) with ROH and/or W present in the probe solvation microsphere. Application of this model requires knowledge of the effective concentrations of the above-mentioned solvent species, based on K_{dissoc} and their exchange equilibria in the solvation microsphere (defined by φ). K_{dissoc} is obtained by iteration from density vs composition data, by use of an equation that calculates V_{ROH-W} and K_{dissoc} simultaneously. This approach may be suspect due to multicollinearity. Reliable values of V_{ROH-W} may be obtained by *ab initio* calculations, corrected for the nonideality of the binary solvent mixtures at different temperatures. The COSMO-RS solvation model gave better fit to the density data than the IEFPCM model. V_{ROH-W} is then employed as a constant in the

equation employed to calculate K_{dissoc}; the latter furnishes effective concentrations of the solvent species present. Information about the solvatochromism of RB in five aqueous alcohols at 25 °C and about its thermosolvatochromism in aqueous ethanol in the temperature range 10−60 °C was obtained from $\chi^{BK;effective}$ and E_T^{obs}. Values of φ can be rationalized in terms of probe−solvent interactions, in particular hydrogen-bonding and hydrophobic interactions with ROH. From the limited data available, the latter interactions seem to be more important. Temperature increase results in a gradual desolvation of RB, due to the concomitant decrease of solvent structure.

List of Abbreviations and Symbols

COSMO-RS: Conductor-like screening model for real solvents.

E_T(probe): Empirical solvent polarity scale of a solvatochromic probe, in kcal mol^{-1}.

E_T(30): Empirical solvent polarity scale of RB, in kcal mol^{-1}.

IEFPCM: Integral equation formalism model.

K_{dissoc}: Dissociation constant of the ROH−W species.

M_{ROH}: Molecular mass of the alcohol ROH.

M_{ROH-W}: Molecular mass of the species ROH−W.

M_W: Molecular mass of water.

RB: 2,6-Diphenyl-4-(2,4,6-triphenylpyridinium-1-yl)phenolate.

ROH−W: 1:1 Alcohol−water hydrogen-bonded species.

V_{SC}: Solvent cavity volumes.

V_M^{SC}: Theoretical molar volumes.

V_M^{Th}: Theoretical molar volumes corrected for temperature.

$V_M^{E,\alpha}$: Excess molar volume as a function of volume fraction.

V_M: Experimental molar volume of the solvent.

V_{ROH}: Experimental molar volume of alcohol.

V_W: Experimental molar volume of water.

V_{ROH-W}: Molar volume of the hydrogen-bonded alcohol−water species, corrected for temperature and nonideality of the binary solvent mixture.

α: Volume fraction scale.

χ: Mole fraction scale.

φ: Solvent fractionation factor.

ρ: Solution density.

Acknowledgment. We thank FAPESP (State of São Paulo Research Foundation) for financial support, predoctoral fellowship to P.L.S., and postdoctoral fellowship to E.L.B. and CNPq (National Council for Scientific and Technological Research) for a research productivity fellowship to O.A.E-S. We thank Clarissa T. Martin and Michelle S. Lima for their help and the LCCA laboratory for making the programs and computation facilities available to us.

Supporting Information Available: Plot of B3LYP/6-31+G(3d,p) optimized geometries of water−alcohol hydrogen-bonded complexes; plot showing the application of the van't Hoff equation to K_{dissoc} of the alcohols studied; table of corrected molar volume of 1:1 water−alcohol complexes, obtained with PCM using a B3LYP/6-31+G(3d,p) basis set. This material is available free of charge via the Internet at http://pubs.acs.org.

References and Notes

(1) Reichardt, C. *Solvents and Solvent Effects in Organic Chemistry*, 3rd ed.; Wiley-VCH: Weinheim, Germany, 2003; pp 147 and 389 and references therein.

(2) Reichardt, C. *Pure Appl. Chem.* **2004**, *76*, 1903.

(3) Tada, E. B.; Silva, P. L.; El Seoud, O. A. *J. Phys. Org. Chem.* **2003**, *16*, 691.

(4) Tada, E. B.; Silva, P. L.; El Seoud, O. A. *Phys. Chem. Chem. Phys.* **2003**, *5*, 5378.

(5) Tada, E. B.; Silva, P. L.; Tavares, C.; El Seoud, O. A. *J. Phys. Org. Chem.* **2005**, *18*, 398.

(6) Katz, E. D.; Ogan, K.; Scott, R. P. W. *J. Chromatogr.* **1986**, *352*, 67.

(7) Katz, E. D.; Lochmuller, C. H.; Scott, R. P. W. *Anal. Chem.* **1989**, *61*, 349.

(8) Scott, R. P. W. *Analyst* **2000**, *125*, 1543.

(9) Draper, N. R.; Smith, H. *Applied Regression Analysis*, 3rd ed.; Wiley-Interscience: New York, 1998.

(10) Shimizu, S.; Pires, P. A. R.; El Seoud, O. A. *Langmuir* **2003**, *19*, 9645.

(11) Tada, E. B. Solvatochromism in solvents and in micellar systems. Ph.D. Thesis, University of São Paulo, São Paulo, Brazil, 2004.

(12) Mikhail, S. Z.; Kimel, W. R. *J. Chem. Eng. Data* **1963**, *8*, 323.

(13) Lee, C.; Yang, W.; Parr, R. G. *Phys. Rev. B: Condens. Matter Mater. Phys.* **1988**, *37*, 785.

(14) Becke, A. D. *J. Chem. Phys.* **1993**, *98*, 5648.

(15) Cancès, M. T.; Mennucci, B.; Tomasi, J. *J. Chem. Phys.* **1997**, *107*, 3032.

(16) Tomasi, J.; Mennucci, B.; Cancès, M. T. *J. Mol. Struct.* **1999**, *464*, 211.

(17) Eckert, F.; Klamt, A. *AIChE J.* **2002**, *48*, 369.

(18) Frisch, M. J.; Trucks, G. W.; Schlegel, H. B.; Scuseria, G. E.; Robb, M. A.; Cheeseman, J. R.; Montgomery, J. A., Jr.; Vreven, T.; Kudin, K. N.; Burant, J. C.; Millam, J. M.; Iyengar, S. S.; Tomasi, J.; Barone, V.; Mennucci, B.; Cossi, M.; Scalmani, G.; Rega, N.; Petersson, G. A.; Nakatsuji, H.; Hada, M.; Ehara, M.; Toyota, K.; Fukuda, R.; Hasegawa, J.; Ishida, M.; Nakajima, T.; Honda, Y.; Kitao, O.; Nakai, H.; Klene, M.; Li, X.; Knox, J. E.; Hratchian, H. P.; Cross, J. B.; Bakken, V.; Adamo, C.; Jaramillo, J.; Gomperts, R.; Stratmann, R. E.; Yazyev, O.; Austin, A. J.; Cammi, R.; Pomelli, C.; Ochterski, J. W.; Ayala, P. Y.; Morokuma, K.; Voth, G. A.; Salvador, P.; Dannenberg, J. J.; Zakrzewski, V. G.; Dapprich, S.; Daniels, A. D.; Strain, M. C.; Farkas, O.; Malick, D. K.; Rabuck, A. D.; Raghavachari, K.; Foresman, J. B.; Ortiz, J. V.; Cui, Q.; Baboul, A. G.; Clifford, S.; Cioslowski, J.; Stefanov, B. B.; Liu, G.; Liashenko, A.; Piskorz, P.; Komaromi, I.; Martin, R. L.; Fox, D. J.; Keith, T.; Al-Laham, M. A.; Peng, C. Y.; Nanayakkara, A.; Challacombe, M.; Gill, P. M. W.; Johnson, B.; Chen, W.; Wong, M. W.; Gonzalez, C.; Pople, J. A. *Gaussian 03*, revision C.02; Gaussian, Inc.: Wallingford, CT, 2004.

(19) Thompson, M. A. 4.0.1 ed.; Planaria Software LLC: Seattle, WA, 2005.

(20) Antonious, M. S.; Tada, E. B.; El Seoud, O. A. *J. Phys. Org. Chem.* **2002**, *15*, 403.

(21) Rosés, M.; Ràfols, C.; Ortega, J.; Bosch, E. *J. Chem. Soc., Perkin Trans. 2* **1995**, 1607.

(22) Bosch, E.; Rosés, M. *J. Phys. Org. Chem.* **1996**, *9*, 403.

(23) Ortega, J.; Ràfols, C.; Bosch, E.; Rosés, M. *J. Chem. Soc., Perkin Trans. 2* **1996**, 1497.

(24) Bosch, E.; Rived, F.; Rosés, M. *J. Chem. Soc., Perkin Trans. 2* **1996**, 2177.

(25) Ràfols, C.; Rosés, M.; Bosch, E. *J. Chem. Soc., Perkin Trans. 2* **1997**, 243.

(26) Buhvestov, U.; Rived, F.; Ràfols, C.; Bosch, E.; Rosés, M. *J. Phys. Org. Chem.* **1998**, *11*, 185.

(27) Roux, G.; Roberts, D.; Perron, G.; Desnoyers, J. E. *J. Solution Chem.* **1980**, *9*, 629.

(28) Zana, R.; Eliebari, M. J. *J. Phys. Chem.* **1993**, *97*, 11134.

(29) Sacco, A.; De Cillis, F. M.; Holz, M. *J. Chem. Soc., Faraday Trans.* **1998**, *94*, 2089.

(30) Harris, K. R.; Newitt, P. J. *J. Phys. Chem. A* **1999**, *103*, 6508.

(31) Petong, P.; Pottel, R.; Kaatze, U. *J. Phys. Chem. A* **2000**, *104*, 7420.

(32) Nishikawa, K.; Hayashi, H.; Iijima, T. *J. Phys. Chem.* **1989**, *93*, 6559.

(33) Huelsekopf, M.; Ludwig, R. *J. Mol. Liq.* **2000**, *85*, 105.

(34) Marcus, Y. *Monatsh. Chem.* **2001**, *132*, 1387 and references therein.

(35) Chen, J.-S.; Shiao, J.-C. *J. Chem. Soc., Faraday Trans.* **1994**, *90*, 429.

(36) Eblinger, F.; Schneider, H.-J. *J. Phys. Chem.* **1996**, *100*, 5533.

(37) Max, J. J.; Daneault, S.; Chapados, C. *Can. J. Chem.* **2002**, *80*, 113.

(38) Coetzee, J. F.; Hussam, A. *J. Solution Chem.* **1982**, *11*, 395.

(39) Rablen, P. R.; Lockman, J. W.; Jorgensen, W. L. *J. Phys. Chem. A* **1998**, *102*, 3782.

(40) Stockman, P. A.; Blake, G. A.; Lovas, F. J.; Suenram, R. D. *J. Chem. Phys.* **1997**, *107*, 3782.

(41) Schowen, R. L. *Transition States of Biochemical Processes*; Plenum Press: New York, 1978.

(42) Anslyn, E. V.; Dougherty, D. A. *Modern Physical Organic Chemsitry*; University Science Books: Sausalito, CA, 2004.

(43) Wensink, E. J. W.; Hoffmann, A. C.; van Maaren, P. J.; van der Spoel, D. *J. Chem. Phys.* **2003**, *119*, 7308.
(44) Tomasi, J.; Mennucci, B.; Cammi, R. *Chem. Rev.* **2005**, *105*, 2999.
(45) Lunelli, B.; Scagnolari, F. *J. Chem. Educ.* **2002**, *79*, 626.
(46) Mori, H.; Iwata, S.; Kawachi, T.; Matsubara, T.; Nobuoka, Y.; Aragaki, T. *J. Chem. Eng. Jpn.* **2004**, *37*, 850.
(47) Kusano, K.; Suurkuus, J.; Wadso, I. *J. Chem. Thermodyn.* **1973**, *5*, 757.
(48) Davis, M. I.; Molina, M. C.; Douheret, G. *Thermochim. Acta* **1998**, *317*, 105.
(49) Tamura, K.; Tabata, S.; Murakami, S. *J. Chem. Thermodyn.* **1998**, *30*, 1319.
(50) Kaatze, U.; Pottel, R.; Schumacher, A. *J. Phys. Chem.* **1992**, *96*, 6017.
(51) Brai, M.; Kaatze, U. *J. Phys. Chem.* **1992**, *96*, 8946.
(52) Kaatze, U.; Schumacher, A.; Pottel, R. *Ber. Bunsen-Ges. Phys. Chem.* **1991**, *95*, 585.
(53) Dawber, J. G.; Williams, R. A. *J. Chem. Soc., Faraday Trans.* **1986**, *82*, 3097.
(54) Barlin, G. B.; Perrin, D. D. *Q. Rev.* **1966**, *20*, 75.
(55) Kingston, B.; Symons, M. C. R. *J. Chem. Soc., Faraday Trans.* **1973**, *69*, 978.
(56) Symons, M. C. R. *Pure Appl. Chem.* **1986**, *58*, 1121.
(57) Haak, J. R.; Engberts, J. *Recl. Trav. Chim. Pays-Bas* **1986**, *105*, 307.
(58) Shulgin, I.; Ruckenstein, E. *J. Phys. Chem. B* **1999**, *103*, 2496.
(59) Shulgin, I.; Ruckenstein, E. *J. Phys. Chem. B* **1999**, *103*, 872.